Revista ALCONPAT
www.revistaalconpat.org
eISSN 2007-6835
Revista de la Asociación Latinoamericana de Control de Calidad, Patología y Recuperación de la Construcción

Multi-response optimization of flowability and compressive strength in alkali-activated slag mortar using Taguchi–PCR-TOPSIS approach.

A. A. Adam[1]*, B. R. Ramadhan[1], I. H. Emeraldy[1], A. P. Kasim[1]
*Contact author: andi.arham@untad.ac.id
DOI: https://doi.org/10.21041/ra.v16i3.1035

Received: 28/03/2026 | Received in revised form: 09/08/2026 | Accepted: 26/08/2026 | Published: 01/09/2026

ABSTRACT
This study aimed to identify an Alkali-Activated Slag (AAS) mortar mixture balancing flowability and compressive strength as a sustainable alternative to Portland cement. Twenty-seven mixtures varying activator dosage, modulus, water-to-binder ratio, aggregate-to-binder ratio, and superplasticizer content were evaluated using a Taguchi L27 design, ANOVA, and PCR-TOPSIS optimization. Activator dosage was most influential (70.90% contribution), followed by aggregate-to-binder ratio (10.12%), while modulus and water-to-binder ratio played minor roles. The optimal mixture (flow 115%, strength 48.85 MPa) was validated by an independent replicate batch, with an estimated 79% lower CO_2 footprint than a Portland-cement control. Reaction mechanisms were not confirmed microstructurally. Unlike prior single-response approaches, this study combines statistical validation, experimental confirmation, and environmental estimation for a more rigorous mortar design basis.
Keywords: alkali-activated slag; multi-response optimization; PCR–TOPSIS; Taguchi method; compressive strength; flowability.

Cite as: Adam, A. A., Ramadhan, B. R., Emeraldy, I. H., Kasim, A. P. (2026), "*Multi-response optimization of flowability and compressive strength in alkali-activated slag mortar using Taguchi–PCR-TOPSIS approach*.", Revista ALCONPAT, 16 (3), pp. 475 – 492, DOI: https://doi.org/10.21041/ra.v16i3.1035

[1] Faculty of Engineering, Tadulako University,Palu/ Central of Sulawesi, 94118, Indonesia.

Contribution of each author
In this work, author A contributed with activity X, author B contributed with activity Y, and so on; being activities X, Y, etc., those related to the contributions offered to the manuscript: original idea, experimentation, development of a model, data collection, writing of the work, discussion of results, or others.

Discussions and subsequent corrections to the publication
Any dispute, including the replies of the authors, will be published in the second issue of 2027 provided that the information is received before the closing of the first issue of 2027.

Optimización multi-respuesta de la fluidez y la resistencia a la compresión en morteros de escoria activada alcalinamente mediante el enfoque Taguchi–PCR-TOPSIS.

RESUMEN

Este estudio tuvo como objetivo identificar una mezcla de mortero de escoria activada alcalinamente (AAS) que equilibre la fluidez y la resistencia a la compresión como alternativa sostenible al cemento Portland. Se evaluaron veintisiete mezclas variando la dosificación del activador, el módulo, la relación agua/ligante, la relación agregada/ligante y el contenido de superplastificante mediante un diseño Taguchi L27, ANOVA y optimización PCR-TOPSIS. La dosificación del activador fue el parámetro más influyente (70.90% de contribución), seguido por la relación agregado/ligante (10.12%), mientras que el módulo y la relación agua/ligante desempeñaron roles menores. La mezcla óptima (fluidez 115%, resistencia 48.85 MPa) fue validada mediante un lote réplica independiente, con una huella de CO_2 estimada 79% menor que un control de cemento Portland. Los mecanismos de reacción no fueron confirmados microestructuralmente. A diferencia de los enfoques de respuesta única previos, este estudio combina validación estadística, confirmación experimental y estimación ambiental para una base de diseño de mortero más rigurosa.

Palabras clave: escoria activada alcalinamente; optimización multi-respuesta; PCR–TOPSIS; método Taguchi; resistencia a la compresión; fluidez.

Otimização multi-resposta da fluidez e da resistência à compressão em argamassas de escória ativada alcalinamente através da abordagem Taguchi–PCR-TOPSIS.

RESUMO

Este estudo teve como objetivo identificar uma mistura de argamassa de escória ativada alcalinamente (AAS) que equilibre a fluidez e a resistência à compressão como alternativa sustentável ao cimento Portland. Foram avaliadas vinte e sete misturas variando a dosagem do ativador, o módulo, a relação água/aglomerante, a relação agregado/aglomerante e o teor de superplastificante, por meio de um planejamento Taguchi L27, ANOVA e otimização PCR-TOPSIS. A dosagem do ativador foi o parâmetro mais influente (70,90% de contribuição), seguido pela relação agregado/aglomerante (10,12%), enquanto o módulo e a relação água/aglomerante desempenharam papéis menores. A mistura ótima (fluidez 115%, resistência 48,85 MPa) foi validada por meio de um lote réplica independente, com uma pegada de CO2 estimada 79% menor que um controle de cimento Portland. Os mecanismos de reação não foram confirmados microestruturalmente. Diferentemente das abordagens de resposta única anteriores, este estudo combina validação estatística, confirmação experimental e estimativa ambiental para uma base de projeto de argamassa mais rigorosa.

Palavras-chave: escória ativada alcalinamente; otimização multi-resposta; PCR–TOPSIS; método Taguchi; resistência à compressão; fluidez.

Legal Information

Revista ALCONPAT is a quarterly publication by the Asociación Latinoamericana de Control de Calidad, Patología y Recuperación de la Construcción, Internacional, A.C., Km. 6 antigua carretera a Progreso, Mérida, Yucatán, 97310, Tel. +52 1 983 419 8241, alconpat.int@gmail.com, Website: www.alconpat.org

Reservation of rights for exclusive use No.04-2013-011717330300-203, and ISSN 2007-6835, both granted by the Instituto Nacional de Derecho de Autor. Responsible editor: Pedro Castro Borges, Ph.D. Responsible for the last update of this issue, Informatics Unit ALCONPAT, Elizabeth Sabido Maldonado.

The views of the authors do not necessarily reflect the position of the editor.

1. INTRODUCTION

The rapid expansion of infrastructure development has significantly increased the demand for cement-based materials, leading to serious environmental concerns. Ordinary Portland cement (OPC) production is associated with high energy consumption and substantial carbon dioxide (CO_2) emissions, reaching approximately 0.9 tons of CO_2 per ton of cement produced (Qaidi et al., 2022). This issue has become increasingly critical in developing countries such as Indonesia, where infrastructure growth continues to accelerate.

In recent years, Indonesia—particularly Central Sulawesi—has experienced rapid industrial expansion, especially in the steel sector. The development of steel-processing industries has resulted in the large-scale generation of industrial by-products such as ground granulated blast furnace slag (GGBFS). The effective utilization of these by-products is essential to reduce environmental burdens while supporting sustainable construction practices. Alkali-activated slag (AAS) materials have emerged as a promising alternative binder, utilizing GGBFS activated by alkaline solutions to produce low-carbon cementitious systems with favorable mechanical and durability properties (Cong et al., 2024), (Kaliyavaradhan et al., 2024).

Previous studies have demonstrated that AAS materials can achieve high compressive strength and enhanced durability compared to conventional cement systems, making them suitable for structural applications (Cong et al., 2024),(Zhang et al., 2022). However, most existing research primarily focuses on mechanical performance, particularly compressive strength, as the main indicator of material quality. In practical applications, the performance of mortar is not solely governed by strength but also by workability, which significantly affects casting, compaction, and overall constructability.

Despite its importance, limited studies have addressed the interaction between workability and strength in AAS mortar systems. In many cases, increasing compressive strength leads to reduced flowability, indicating the existence of a trade-off between these two properties. This condition highlights the need for a more comprehensive evaluation approach that considers multiple performance criteria simultaneously. Nevertheless, most studies still rely on single-response optimization, which may not adequately represent real engineering requirements.

Furthermore, the application of systematic multi-response optimization methods in AAS research remains relatively limited. Advanced techniques such as Taguchi-based optimization combined with multi-response decision-making methods offer a more effective approach for identifying optimal mix compositions that balance competing properties.

Therefore, this study aims to investigate the combined effects of mix composition on flow and compressive strength of alkali-activated slag mortar using a Taguchi experimental design. A multi-response optimization approach based on PCR-TOPSIS is employed to determine the optimal mixture proportion that simultaneously satisfies workability and mechanical performance requirements. The outcomes of this study are expected to contribute to the development of sustainable construction materials utilizing industrial by-products, particularly in rapidly developing regions such as Indonesia.

2. EXPERIMENTAL

2.1 Materials and method.

A statistical experimental design based on the Taguchi method was employed to evaluate the influence of mix composition on the performance of alkali-activated slag (AAS) mortar. The Taguchi approach enables efficient optimization by reducing the number of experimental trials while maintaining the ability to analyze multiple factors simultaneously through orthogonal arrays (Taguchi, 1990) In this study, an L27 (3^5) orthogonal array was adopted to accommodate five control factors, each at three levels. The selected factors include activator dosage (4%, 5%, and 6%), modulus (0.8, 1.0, and 1.2), water-to-binder ratio (0.46, 0.47, and 0.48), aggregate-to-binder ratio (2.25, 2.50, and 2.75), and superplasticizer content (1%, 2%, and 3%). These variables were selected due to their significant influence on both workability and mechanical performance of AAS mortar systems (Cong et al., 2024), (Amer et al., 2021), (J. L. Provis, 2018). The activator dosage (D) refers to the percentage of alkaline solution relative to the binder mass, which controls the availability of reactive species for the geopolymerization process. A higher dosage generally enhances the dissolution of aluminosilicate precursors, leading to increased formation of binding gels and improved mechanical strength(Law et al., 2012). The modulus (M), defined as the ratio of SiO_2 to Na_2O in the alkaline solution, represents the silica availability within the activator system(Law et al., 2012). This parameter plays a critical role in governing the formation of C-(A)-S-H gel and influences both the workability and strength development of alkali-activated slag mortar. The experimental design was analyzed using signal-to-noise (S/N) ratio and analysis of variance (ANOVA), followed by multi-response optimization using the PCR-TOPSIS method to determine the optimal mixture proportion considering both flow and compressive strength.

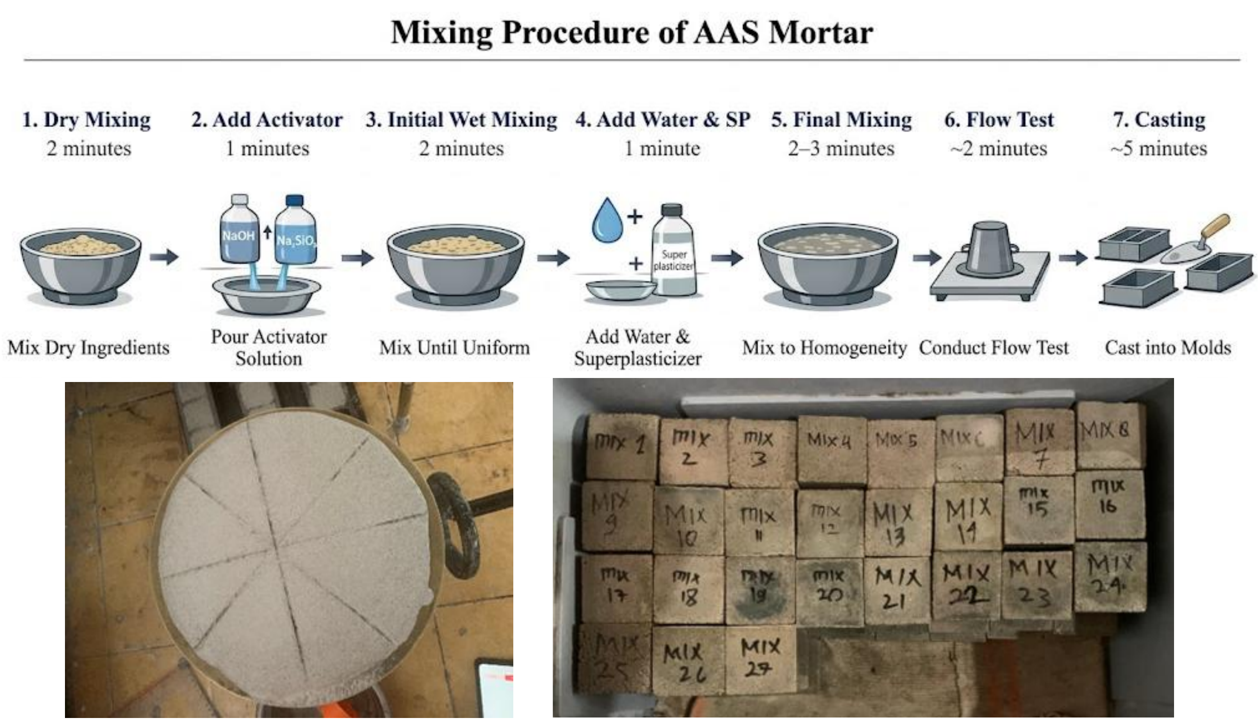

Figure 1. a) Mixing Procedure AAS Mortar, b) Flow Process, c) Mortars.

Mortar specimens were prepared using ground granulated blast furnace slag (GGBFS) as the primary binder as shown in Table 1 and Figure 1, conforming to ASTM C989/C989M (ASTM International, 2022), and activated by a combination of sodium hydroxide (NaOH) and sodium silicate (Na_2SiO_3)(Nath & Sarker, 2014)(Amer et al., 2021). Local river sand, conforming to ASTM C33/C33M (ASTM International, 2018), with a fineness modulus of 2.48 was used as fine aggregate. The mixing process was carried out using a mechanical mixer to ensure uniformity. Initially, GGBFS and fine aggregate were dry-mixed for approximately 2 minutes. Subsequently, the alkaline solution and superplasticizer were added gradually, and mixing was continued until a homogeneous and workable mortar was obtained. The fresh mortar was then cast into cube molds and compacted to eliminate entrapped air. After casting, the specimens were covered to minimize moisture loss prior to curing.

Table 1. Chemical Compositions of GGBFS and PCC based on XRF test.

Material	CaO	SiO_2	Al_2O_3	MgO	TiO_2	MnO	S	K_2O	Fe_2O_3	Na_2O	SO_3	LOI
GGBFS	41.56	37.42	15.20	1.24	0.71	0.30	0.75	0.36	0.52	0.51	1.88	0.65
Cement (PCC)	55.00	25.00	8.00	2.50	–	–	–	0.80	4.00	–	2.50	1.50

The workability of the fresh mortar was evaluated using the flow table test in accordance with ASTM C1437 (ASTM International, 2020). The test was performed by subjecting the mortar to 25 drops within 15 seconds, and the flow value was determined as the percentage increase in the average diameter of the spread mortar. Compressive strength testing was carried out in accordance with ASTM C109/C109M (ASTM International, 2023) using cube specimens with dimensions of 50 mm × 50 mm × 50 mm. The tests were conducted at curing ages of 7 and 28 days to evaluate both early-age and standard mechanical performance. These curing periods are commonly adopted for assessing the strength development of cementitious materials (Farooq et al., 2021), (ASTM International, 2023).

Table 2. AASM Mix Design

Code	Dosage (%)	Modulus	W/B	Agg/B	SP (%)	Code	D (%)	M	W/B	Agg/B	SP (%)
T408046225	4	0.8	0.46	2.25	1	T510048225	5	1.0	0.48	2.25	1
T408047250	4	0.8	0.47	2.50	2	T510046250	5	1.0	0.46	2.50	2
T408048275	4	0.8	0.48	2.75	3	T510047275	5	1.0	0.47	2.75	3
T410046250	4	1.0	0.46	2.50	3	T512048250	5	1.2	0.48	2.50	2
T410047275	4	1.0	0.47	2.75	1	T512046275	5	1.2	0.46	2.75	3
T410048225	4	1.0	0.48	2.25	2	T512047225	5	1.2	0.47	2.25	1
T412046275	4	1.2	0.46	2.75	2	T608048275	6	0.8	0.48	2.75	1
T412047225	4	1.2	0.47	2.25	3	T608046225	6	0.8	0.46	2.25	2
T412048250	4	1.2	0.48	2.50	1	T608047250	6	0.8	0.47	2.50	3
T508046250	5	0.8	0.46	2.50	2	T610048225	6	1.0	0.48	2.25	3
T508047275	5	0.8	0.47	2.75	3	T610046250	6	1.0	0.46	2.50	1
T508048225	5	0.8	0.48	2.25	1	T610047275	6	1.0	0.47	2.75	2
T510046275	5	1.0	0.46	2.75	3	T612048250	6	1.2	0.48	2.50	3
T510047225	5	1.0	0.47	2.25	1	CMPCC	-	-	0.47	2.50	2

A confirmation mix using conventional Portland Composite Cement (PCC) was prepared as a control specimen, designed to achieve a target compressive strength of 25.231 MPa at 28 days. The mix proportion consisted of a water-to-binder ratio of 0.47, an aggregate-to-binder ratio of 2.50, and 2% superplasticizer. This control mix was used for comparison with alkali-activated slag mortar in terms of workability and compressive strength.
To ensure a fair basis of comparison between the AAS mixtures and the CMPCC control, the water-to-binder ratio (0.47), aggregate-to-binder ratio (2.50), and superplasticizer dosage (2%) of the CMPCC control were deliberately matched to the mid-level values used in the AAS mix design (Table 2), rather than being independently optimized. It should be noted, however, that the water-to-binder ratio reported in Table 2 for the AAS mixtures (0.46-0.48) reflects only the added mixing water and does not include the water contained within the NaOH and Na2SiO3 activator solutions. When this additional water is accounted for, the effective total water-to-binder ratio of the AAS mixtures is estimated to range from approximately 0.49 to 0.52 (e.g., approximately 0.50 for the optimal mixture T610046250), based on the activator solution compositions described in Section 2.3. This is somewhat higher than the nominal water-to-binder ratio of the CMPCC control (0.47) and is an inherent characteristic of alkali-activated systems, where a portion of the mixing liquid is supplied through the activator rather than as free water, consistent with observations in previous AAS studies [8],[6]. Readers should therefore weigh the reported compressive strength and workability comparisons between AAS and CMPCC mixtures against this difference in effective water content, rather than assuming identical water availability between the two binder systems.
After casting, the specimens were covered with plastic sheets to minimize moisture loss and kept at ambient laboratory temperature (±25 °C) for 24 hours. Subsequently, the specimens were demolded and cured under ambient conditions until the testing ages of 7 and 28 days. This curing regime was adopted to simulate practical field conditions and to evaluate the performance of alkali-activated slag mortar under non-controlled curing environments.

2.2 Multi-response optimization and statistical analysis

To evaluate the influence of mix parameters and determine the optimal mixture composition, statistical analysis and multi-response optimization were conducted using Analysis of Variance (ANOVA) and the PCR–TOPSIS method.
ANOVA was applied to quantify the contribution of each factor to the variation in compressive strength(Taguchi, 1990). The percentage contribution of each parameter was calculated based on the ratio of its sum of squares to the total sum of squares, as expressed in Eq. (1):

$$P_i = \frac{SS_i}{SS_{total}} x100\% \tag{1}$$

where P_i_is the percentage contribution of factor i, SS_i is the sum of squares of factor i, and $SS_{total}$is the total sum of squares. For multi-response optimization, the PCR–TOPSIS method was employed to simultaneously evaluate flowability and compressive strength(Jolliffe, 2002)(Hwang & Yoon, 1981)(Behzadian et al., 2012)(Madanchian & Taherdoost, 2023). The decision matrix $X_{ij}$was first normalized using vector normalization to eliminate differences in measurement units Eq. (2):

$$r_{ij} = \frac{X_{ij}}{\sqrt{\sum_{i=1}^{m} X_{ij}^2}} \tag{2}$$

The normalized matrix was then weighted to reflect the relative importance of each response Eq.(3):

$$v_{ij} = w_j . r_{ij} \tag{3}$$

where w_j represents the weight of each response. The ideal best A^+ and ideal worst A^- solutions were defined based on the maximum and minimum values of the weighted normalized matrix. The separation distances from the ideal solutions were calculated as Eq.(4) and Eq.(5):

$$D_i^+ = \sqrt{\sum_{j=1}^{n} (v_{ij} - v_j^+)^2} \tag{4}$$

$$D_i^- = \sqrt{\sum_{j=1}^{n} (v_{ij} - v_j^-)^2} \tag{5}$$

Finally, the relative closeness coefficient (C_i) was determined using Eq.(6) :

$$C_i = \frac{D_i^-}{D_i^+ + D_i^-} \tag{6}$$

The alternative with the highest C_i value was considered the optimal mixture. This approach enables the identification of a balanced solution when multiple performance criteria exhibit conflicting behavior.

2.3 CO_2 emission estimation.

Cradle-to-gate CO2 emission estimate was performed for each of the 27 AAS mixtures and for the CMPCC control, based on published emission factors and the mix design proportions in Table 2. The following emission factors were adopted: GGBFS = 0.143 kg CO2/kg (Ahmad et al., 2022); NaOH (solid basis) = 1.915 kg CO2/kg [20]; Na2SiO3 solution (as supplied) = 1.222 kg CO2/kg (Turner & Collins, 2013); polycarboxylate ether (PCE) superplasticizer = 2.25 kg CO2/kg dry polymer (Schiefer & Plank, 2023); and ordinary Portland cement (OPC, used in CMPCC) = 0.91 kg CO2/kg (Ahmad et al., 2022).

Because the alkaline activator solution used in this study (10 M NaOH and extra-pure Na2SiO3, Na2O 7.5-8.5%, SiO2 25.5-28.5%) was not chemically characterized for CO2 accounting purposes in the original experimental program, the following assumptions were adopted for this estimate: (1) the NaOH solution mass fraction was taken as 30% (10 M solution, density approx. 1.33 g/mL); (2) the Na2SiO3 solution composition was taken as the midpoint of the supplier specification (Na2O = 8%, SiO2 = 27%); (3) the modulus (M) was treated as the SiO2/Na2O mass ratio of the combined activator, and the activator dosage (D, %) was treated as the total activator solution mass relative to the GGBFS binder mass, and (4) the PCE-based superplasticizer (Sika) was assumed to have a solids content of 30%, typical of commercial polycarboxylate admixtures. These assumptions allow the relative mass proportions of NaOH solution and Na2SiO3 solution required to satisfy each mixture's D and M values to be back-calculated, and the corresponding CO2 emissions to be estimated on a basis of 1 kg of binder.

3. RESULT AND DISCUSSION

3.1 Workability performance (flow analysis).

The workability of alkali-activated slag (AAS) mortar was evaluated using the flow table test, and the results are summarized in Figure 2. The experimental results indicate that the flow values varied significantly across different mix compositions, ranging from approximately 49% to 135.25%, demonstrating the strong influence of activator composition and mixture proportions on fresh-state behavior.

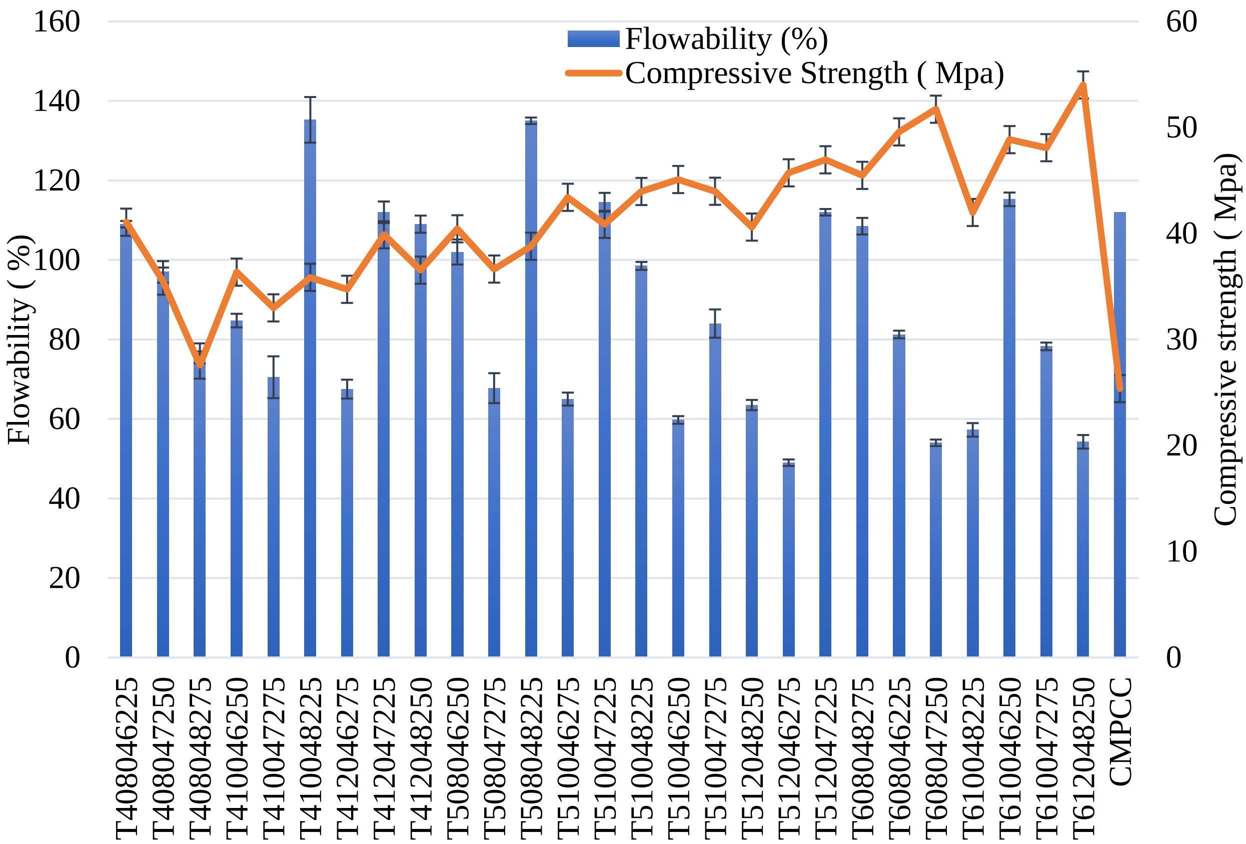

Figure 2 Flowability and 28-Day Compressive Strength of AAS Mortar Graph

The maximum flow value obtained in this study reached 135.25%, which exceeds the target range (110 ± 5%). Based on the experimental observations and the supporting analysis presented in Figure 3 , the variation in flow is primarily governed by key parameters such as activator dosage, modulus, and water-to-binder ratio. This finding is consistent with previous studies, which reported that increasing liquid content, including activator and water, enhances particle lubrication and reduces internal friction, thereby improving workability(Duxson et al., 2007), (Fernández-Jiménez & Palomo, 2005).

The effect of individual factors on flowability can be further analyzed through the ANOVA results, particularly the mean response and signal-to-noise ratio (SNR), as illustrated in Figure 3 and 4. The results indicate that activator dosage and water-to-binder ratio are the most influential parameters. Higher activator dosage increases the liquid phase, improving lubrication between particles and resulting in higher flow values. Likewise, an increase in the water-to-binder ratio reduces mixture viscosity and enhances workability, which is consistent with previous studies on alkali-activated materials (Abudawaba et al., 2021)(Sri Sunarsih et al., 2024)(Heshmat et al., 2024).

However, when the flow results are analyzed together with the 28-day compressive strength, a clear inverse tendency can be observed. Mixtures with excessively high flow values (e.g., >130%) tend to exhibit moderate compressive strength, whereas mixtures with lower flow values (approximately 50–70%) achieve higher strength, reaching up to 54.01 MPa. This indicates a trade-off relationship between workability and mechanical performance.

This phenomenon can be attributed to the increase in effective liquid content, which, although beneficial for workability, leads to higher porosity after hardening and consequently reduces strength. Similar trends have been reported in previous studies, where excessive water or activator content results in reduced mechanical performance due to increased pore volume and weaker microstructure (Fernández-Jiménez & Palomo, 2005), (Nath & Sarker, 2014).

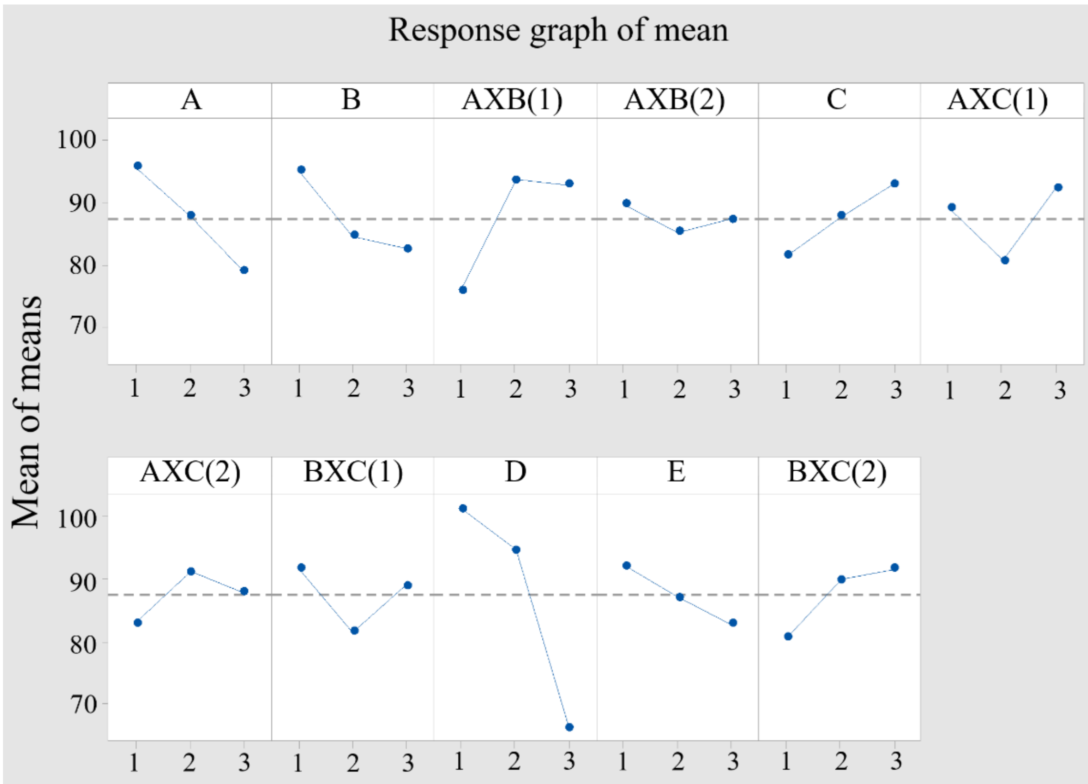

Figure 3. Mean response graphs of AAS mortar flow.

However, excessive flowability is not always desirable. Based on the Taguchi “nominal-the-best” quality characteristic, the flow value should be controlled within a specific target range rather than maximized(Taguchi, 1990)(Mohebi et al., 2015). The results indicate that although higher flow can be achieved, it does not necessarily correspond to optimal performance. This highlights the need to balance workability and mechanical properties, which will be discussed in the following sections

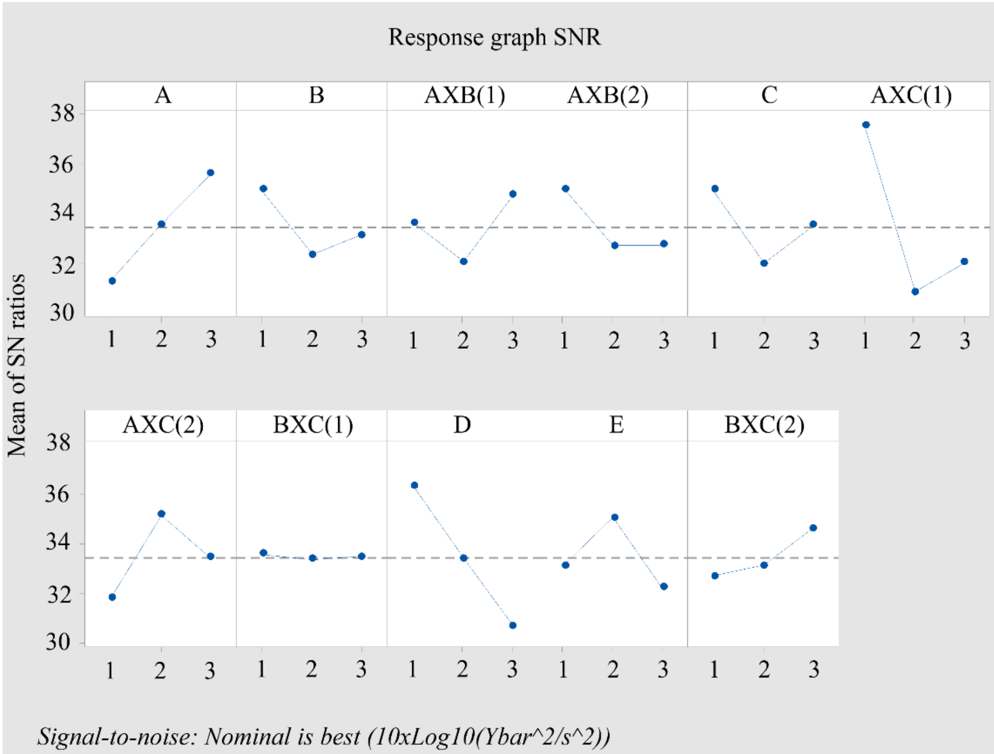

Figure 4. SNR response graphs of AAS mortar flow.

3.2 Compressive Strength Development.

The compressive strength of alkali-activated slag (AAS) mortar was evaluated at curing ages of 3, 7, and 28 days, and the results are presented in Figure 5. The results demonstrate a significant variation in compressive strength depending on the mix composition, confirming the strong influence of activator parameters and mixture proportions.

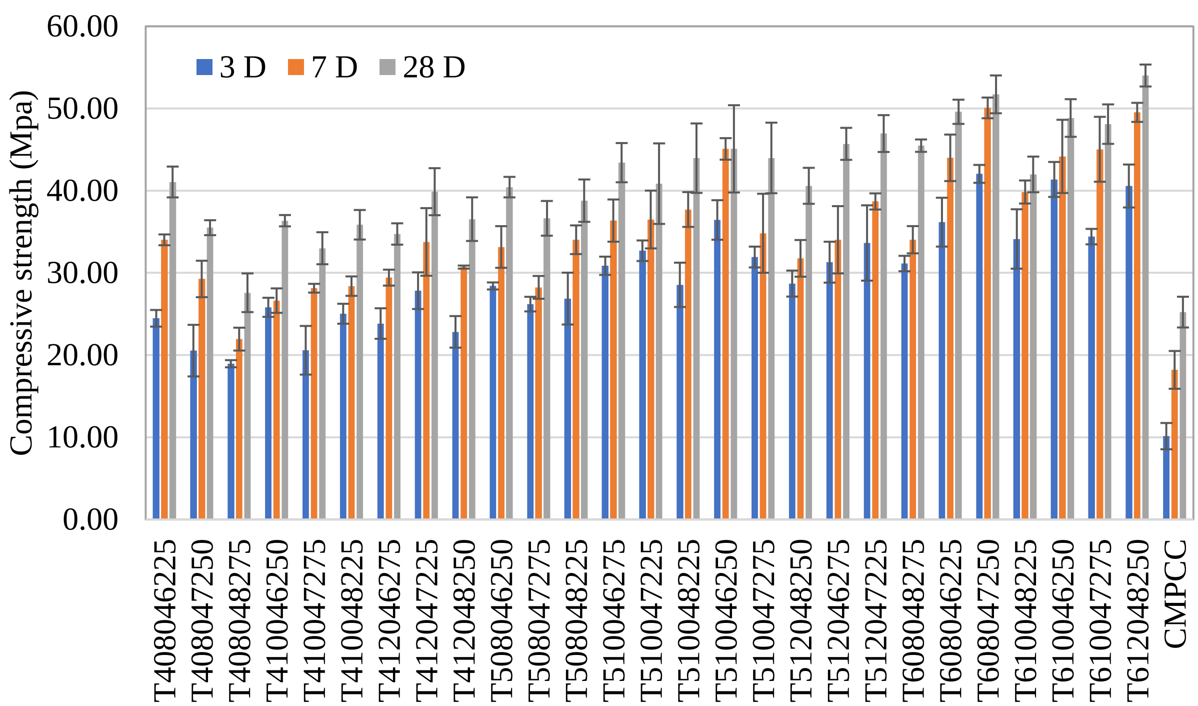

Figure 5. Compressive strength 27 mixtures at 7, 14, 28 days.

At 28 days, the compressive strength ranged from 27.58 MPa (T408048275) to 54.01 MPa (T612048250). The highest strength was achieved by mixture T612048250 (54.01 MPa), followed by T608047250 (51.72 MPa) and T608046225 (49.58 MPa). In contrast, the lowest strength was observed in mixture T408048275 (27.58 MPa). Compared to the control mixture, PCC exhibited a significantly lower strength of 25.36 MPa, confirming that AAS mortar can achieve more than double the compressive strength of conventional mortar. This comparison rests on matched nominal mix ratios (water-to-binder, aggregate-to-binder, and superplasticizer dosage) between the AAS and CMPCC mixtures rather than identical effective water content; see Section 2.1 for a detailed discussion of this distinction.

The strength development with curing time also shows a consistent increasing trend for all mixtures. For instance, mixture T608047250 increased from 42.05 MPa (3 days) to 50.07 MPa (7 days) and reached 51.72 MPa (28 days). Similarly, mixture T510046250 exhibited an increase from 36.44 MPa (3 days) to 45.08 MPa (7 days) and 45.09 MPa (28 days), indicating rapid early-age strength development, which is a known characteristic of AAS systems [25](Luukkonen et al., 2017).

3.3 Effect of mix parameters based on taguchi analysis.

In this study, the evaluated factors consist of activator dosage (Factor A), modulus or SiO_2/Na_2O ratio (Factor B), water-to-binder ratio (Factor C), aggregate-to-binder ratio (Factor D), and superplasticizer-to-binder ratio (Factor E). Building upon the compressive strength, the influence of mix parameters was further evaluated using the Taguchi method through analysis of variance (ANOVA), mean response, and signal-to-noise ratio (SNR).

The ANOVA results based on Table 3 indicate that activator dosage is the most dominant factor governing compressive strength, with a contribution of approximately 70.90%. This significantly higher contribution compared to other parameters confirms that activator concentration plays a critical role in controlling the geopolymerization process, particularly in enhancing precursor dissolution and promoting the formation of a dense and homogeneous reaction matrix (J. Provis & Deventer, 2014), (Fernández-Jiménez & Palomo, 2005).

The validity of ANOVA depends on three underlying assumptions: independence of observations, normality of residuals, and homogeneity of variance (homoscedasticity). Independence was supported by the experimental design, as each of the 27 mixtures corresponds to a physically distinct batch cast and tested as a separate specimen group, following the L27 orthogonal array. Normality of residuals was assessed using the Shapiro-Wilk test applied to the residuals of the fitted main-effects model (observed minus predicted compressive strength for each mixture); the results ($W = 0.971$, $p = 0.629$) indicate no significant departure from normality. Homogeneity of variance was assessed using Levene's test on the residuals grouped by activator dosage ($F = 0.359$, $p = 0.702$) and by modulus ($F = 1.054$, $p = 0.364$); neither test indicated a significant violation of homoscedasticity. The same procedure was applied to the flowability data (Shapiro-Wilk $W = 0.976$, $p = 0.759$; Levene's test by activator dosage $F = 0.385$, $p = 0.685$). As all p-values exceed the 0.05 significance threshold, the assumptions of normality and homogeneity of variance are satisfied for both responses, supporting the appropriateness of ANOVA for this dataset without requiring data transformation.

Table 3. Analysis of variance (ANOVA) table for mean response – fourth iteration.

Source	DOF	Sum of Squares (SS)	Mean Square (MS)	F-ratio
Factor A	2	696.11	348.06	45.20
Factor B	2	62.99	31.49	4.09
Factor C	2	23.37	11.69	1.52
Interaction AC	2	17.13	8.57	1.11
Interaction BC	2	15.01	7.50	0.97
Factor D	2	99.33	49.66	6.45
Factor E	2	12.10	6.05	0.79
Residual Error	12	55.52	4.63	–
Total	26	981.88	–	–

Note: the "Interaction CB" row present in an earlier version of this table has been removed, as it duplicated "Interaction BC" (the B×C and C×B interaction terms are statistically identical). This correction brings the total degrees of freedom to 26, matching the L27 design (27 runs − 1), and the total Sum of Squares to 981.88, consistent with the values reported below.

In contrast, the modulus (SiO_2/Na_2O ratio) exhibits a lower contribution but still influences compressive strength as a secondary parameter. Its effect is associated with the availability of silicate species that contribute to gel formation and structural refinement. However, compared to activator dosage, the contribution of modulus is relatively limited, indicating that its influence is more dependent on interaction with other parameters rather than acting as a primary controlling factor(Nath & Sarker, 2014)(Zheng et al., 2025).
The consistency between mean response and SNR analysis further confirms the robustness of the identified parameter hierarchy in Table 4. The ANOVA results based on SNR also show that activator dosage remains the most significant factor, reinforcing its dominant role in both performance and variability control (Taguchi, 1990)(Mohebi et al., 2015).

Table 4. Analysis of variance (ANOVA) table for snr response – fourth iteration.

Source	Df	SS	MS	F-ratio
A	2	30.49	15.24	53.49
B	2	2.50	1.25	4.39
C	2	1.32	0.66	2.31
AC	2	0.96	0.48	1.68
BC	2	1.15	0.57	2.01
D	2	5.43	2.71	9.52
E	2	0.87	0.43	1.52
Residual Error	12	2.14	0.18	-
Total	26	44.85	-	-

Overall, the Taguchi analysis demonstrates that compressive strength in AAS mortar is primarily controlled by activator dosage, contributing 70,90% of the total variation, while modulus acts as a secondary parameter that influences the efficiency of the reaction system. These findings emphasize that optimization of AAS mortar should prioritize activator concentration, followed by careful adjustment of modulus to achieve a balanced reaction environment(Hardjito et al., 2005).

3.4 Trade-off analysis between flowability and compressive strength.

A trade-off relationship between flowability and compressive strength was observed in alkali-activated slag (AAS) mortar systems, reflecting the competing influence of mix parameters on fresh and hardened properties. Higher flowability is generally associated with increased water-to-binder ratio and optimized activator composition; however, this leads to reduced matrix density and lower compressive strength. Similar trends have been widely reported, where higher water content increases porosity and weakens mechanical performance (J. L. Provis, 2018), (Nath & Sarker, 2014).

Conversely, higher compressive strength is achieved at lower water content and optimal activator conditions, particularly at a dosage of 6% and modulus of 1.2. The role of activator concentration in enhancing reaction kinetics and matrix densification has been well established (Fernandez-Jimenez et al., 2007), .

This inverse relationship indicates that improved workability often comes at the expense of strength. Excessive flow beyond the target range (110 ± 5%) reflects a diluted matrix structure, which may compromise mechanical integrity, as also reported in previous studies (Marvila et al., 2021). Additionally, activator dosage plays a dual role, significantly influencing both strength and flowability under different optimal conditions (Hardjito et al., 2005).

Therefore, the trade-off between flowability and compressive strength highlights the need for multi-response optimization, as both properties cannot be maximized simultaneously. In practice, mix design should be adjusted based on performance requirements, balancing workability and strength to achieve optimal performance.

3.5 Multi-response optimization using PCR–TOPSIS.

To determine the optimal mixture considering both flowability and compressive strength, a multi-response optimization was performed using the PCR–TOPSIS method. The analysis was conducted based on experimental results of flow (%) and 28-day compressive strength (MPa) obtained from the Taguchi design (Hwang & Yoon, 1981)(Behzadian et al., 2012).

The decision matrix was first normalized using vector normalization to eliminate unit differences between responses. Subsequently, weighting factors were assigned based on the relative importance of each response. In this study, compressive strength was assigned a higher weight (0.6) compared to flowability (0.4), considering its dominant contribution as indicated by the ANOVA results. This choice is examined through a sensitivity analysis later in this section (Table 6).

The weighted normalized matrix was then used to determine the ideal best and ideal worst solutions. The separation distances from the ideal solutions were calculated, followed by the determination of the relative closeness coefficient (C_i) for each experimental mixture(Behzadian et al., 2012). The ranking results based on (C_i) are presented in Table 5.

Table 5. Ranking of mix compositions based on multi-response optimization using (C_i)

Mix Code	**Flow (%)**	**Strength (MPa)**	(C_i)	**Rank**
T610046250	115.00	48.85	**0.784**	1
T512047225	112.00	46.95	0.732	2
T608048275	109.00	45.48	0.686	3
T508048225	135.00	38.79	0.655	4
T510047225	115.00	40.86	0.626	5

The results indicate that the optimal mixture is T610046250, which achieved the highest closeness coefficient (Ci) = 0.784. This mixture provides the best balance between flowability and compressive strength, with a flow value of 115% and compressive strength of 48.85 MPa. It is important to note that the optimal mixture identified by the PCR–TOPSIS method differs from the mixture with the highest compressive strength. For instance, mixture T612048250 achieved the maximum compressive strength of 54.01 MPa but exhibited relatively low flowability, resulting in a lower overall ranking.

Similarly, mixtures with excessively high flow values (above 130%) do not necessarily yield optimal performance due to reduced mechanical strength. This confirms the existence of a trade-off relationship between flowability and compressive strength, as previously discussed.

The PCR–TOPSIS method successfully identifies a compromise solution that satisfies both performance criteria simultaneously. Unlike single-response optimization, which may lead to extreme conditions, multi-response optimization provides a more realistic approach for practical engineering applications(Madanchian & Taherdoost, 2023).

To justify the adopted weighting scheme, the PCR–TOPSIS ranking was recalculated under three additional schemes — equal weighting (0.5/0.5), strength-emphasized weighting (0.7/0.3), and an objective Shannon entropy-based weighting (0.21 strength / 0.79 flow) derived from the full 27-mixture dataset — summarized in Table 6.

Table 6. Sensitivity of the PCR–TOPSIS ranking to alternative weighting schemes.

Weighting Scheme	**w (Strength)**	**w (Flow)**	**Rank 1 (Ci)**	**Rank 2 (Ci)**	**Rank 3 (Ci)**
Equal weighting	0.50	0.50	T610046250 (0.777)	T512047225 (0.731)	T508048225 (0.731)
Adopted (subjective)	0.60	0.40	T610046250 (0.784)	T512047225 (0.732)	T608048275 (0.686)
Strength-emphasized	0.70	0.30	T610046250 (0.792)	T512047225 (0.732)	T608048275 (0.683)
Entropy-based (objective)	0.21	0.79	T508048225 (0.911)	T410048225 (0.895)	T610046250 (0.766)

T610046250 remains top-ranked under all subjective schemes, showing the result is not sensitive to reasonable changes in the assigned weights. The entropy-based weighting instead favors flowability because the flow data show greater dispersion, selecting mixtures with flow values (≈135%) outside the target range (110 ± 5%, Section 3.1); since this purely statistical criterion does not reflect engineering priorities, the adopted 0.6/0.4 weighting — supported by the dominant ANOVA contribution of activator dosage to strength (Section 3.3) — is retained.

3.6 Experimental confirmation of the optimal mixture.

To validate the mixture identified as optimal by the PCR-TOPSIS analysis (T610046250), an independent confirmation batch, designated KT610046250, was prepared using the same mix proportions (activator dosage 6%, modulus 1.0, water-to-binder ratio 0.46, aggregate-to-binder ratio 2.50, superplasticizer 1%) and the same curing regime (ambient conditions, 25 degrees C) as the original experimental program. Four replicate specimens were cast and tested at each curing age.

Table 7. Comparison between the original (target) and confirmation (KT610046250) mixture results.

Parameter	Target (T610046250, original)	Confirmed (KT610046250, n = 4)	Deviation (%)	Within ±1 SD of Target?
Flow (%)	115.25 ± 1.71	113.60	−1.43	Yes
Compressive Strength, 7 d (MPa)	41.37 ± 2.13	41.36 ± 0.67	−0.02	Yes
Compressive Strength, 14 d (MPa)	–	45.26 ± 0.90	–	–
Compressive Strength, 28 d (MPa)	48.85 ± 2.29	50.60 ± 0.86	+3.58	Yes

The confirmation results show close agreement with the original target values, with deviations of -1.43% for flow and +3.58% for 28-day compressive strength with 48.85 MPa, both well within the +/-1 standard deviation range of the original measurements and within the commonly applied +/-10% acceptance criterion for Taguchi confirmation experiments (Taguchi, 1990).

3.7 Environmental Impact (CO_2) Estimation

CO_2 emissions across the six AAS mixtures ranged from 0.191 to 0.206 kg CO_2/kg binder, corresponding to a 77.7–79.4% reduction relative to the PCC control (0.924 kg CO_2/kg binder) as stated in Table 8.

Table 8. Estimated CO_2 emissions of representative AAS mixtures and the PCC control.

Mix Code	D (%)	M	CO_2 (kg/kg binder)	Reduction vs. PCC (%)
CMPCC	–	–	0.924	–
T508046250	5	0.8	0.191	79.4
T410046250	4	1.0	0.191	79.3
T510046250	5	1.0	0.191	79.3
T610046250	6	1.0	0.192	79.3
T512046275	5	1.2	0.199	78.5
T612048250	6	1.2	0.206	77.7

This finding is consistent with recent life cycle assessments reporting 70–80% lower carbon emissions for slag- and waste-based geopolymer concretes compared with OPC concrete (Marathe et al., 2025), (Liu et al., 2024). Modulus had a more pronounced effect on emissions than activator dosage: raising the modulus from 0.8 to 1.2 increased emissions by approximately 8% (0.191 to 0.206 kg CO_2/kg binder), reflecting the greater Na_2SiO_3 demand at higher SiO_2/Na_2O ratios, whereas varying dosage from 4% to 6% at a fixed modulus changed emissions by less than 1%. The PCR-TOPSIS-optimal mixture (T610046250) achieved a 79.3% CO_2 reduction relative to PCC, confirming that the mechanically optimal mixture also provides substantial environmental benefit.

4. CONCLUSION

The results show that activator dosage is the most influential parameter governing the compressive strength of alkali-activated slag (AAS) mortar, contributing approximately 70.90% of the total variation, followed by the aggregate-to-binder ratio (10.12%), while modulus (6.42%) and water-to-binder ratio (2.38%) play comparatively minor roles. Taguchi analysis confirms that activator dosage and aggregate proportioning jointly govern strength development, highlighting the importance of optimizing both activator concentration and aggregate content.
The PCR–TOPSIS results indicate that the optimal mixture is not defined by maximum strength or flowability alone, but by a balance between both properties. The optimal mix (T610046250) achieved a flow of 115% and compressive strength of 48.85 MPa. These findings confirm the trade-off between workability and strength and emphasize the importance of multi-response optimization for practical AAS mortar design.
Microstructural characterization (e.g., SEM, XRD, FTIR, or TGA) was not performed in this study. The observed strength trends are broadly consistent with previous studies attributing the mechanical performance of AAS materials to the formation and distribution of C–A–S–H gel and to alkali-activation mechanisms that differ fundamentally from conventional cement hydration. Direct confirmation of these mechanisms in the present mixtures is recommended for future work using microstructural analysis.
The optimal mixture identified through PCR-TOPSIS was validated by an independent replicate batch (KT610046250), confirming the reproducibility of the proposed mix design. This mixture also achieved an estimated 79.3% reduction in CO2 emissions relative to a Portland-cement control, demonstrating that the mechanically optimal AAS mortar also offers substantial environmental benefit. These results support the Taguchi–PCR-TOPSIS framework as an effective approach for developing sustainable, high-performance AAS mortar.

5. REFERENCE

Abudawaba, F., Gomaa, E., Gheni, A., ElGawady, M. (2021). *Developing Mix Proportions for Class C Fly Ash-Based Alkali-Activated 3D-Printed Concrete Mixtures*. Transportation Research Record: Journal of the Transportation Research Board, 2676, 036119812110391. https://doi.org/10.1177/03611981211039167

Ahmad, J., Kontoleon, K. J., Majdi, A., Naqash, M. T., Deifalla, A. F., Ben Kahla, N., Isleem, H. F., Qaidi, S. M. A. (2022). *A Comprehensive Review on the Ground Granulated Blast Furnace Slag (GGBS) in Concrete Production.* Sustainability, 14(14), 8783. https://doi.org/10.3390/su14148783

Amer, I., Kohail, M., El-Feky, M. S., Rashad, A., Khalaf, M. A. (2021). *A review on alkali-activated slag concrete.* Ain Shams Engineering Journal, 12(2), 1475–1499. https://doi.org/https://doi.org/10.1016/j.asej.2020.12.003

Behzadian, M., Khanmohammadi Otaghsara, S., Yazdani, M., Ignatius, J. (2012). *A state-of the-art survey of TOPSIS applications.* Expert Systems with Applications, 39(17), 13051–13069. https://doi.org/https://doi.org/10.1016/j.eswa.2012.05.056

Cong, P., Du, R., Gao, H., Chen, Z. (2024). *Comparison and assessment of carbon dioxide emissions between alkali-activated materials and OPC cement concrete.* Journal of Traffic and Transportation Engineering (English Edition), 11(5), 918–938. https://doi.org/https://doi.org/10.1016/j.jtte.2023.07.011

Duxson, P., Fernández-Jiménez, A., Provis, J., Lukey, G., Palomo, A., Van Deventer, J. (2007). *Geopolymer Technology: The Current State of the Art.* Journal of Materials Science, 42, 2917–2933. https://doi.org/10.1007/s10853-006-0637-z

Farooq, F., Jin, X., Faisal Javed, M., Akbar, A., Izhar Shah, M., Aslam, F., Alyousef, R. (2021). *Geopolymer concrete as sustainable material: A state of the art review.* Construction and Building Materials, 306, 124762. https://doi.org/https://doi.org/10.1016/j.conbuildmat.2021.124762
Fernandez-Jimenez, A., García-Lodeiro, I., Palomo, A. (2007). *Durability of alkali-activated fly ash cementitious materials.* Journal of Materials Science, 42(9), 3055–3065. https://doi.org/10.1007/s10853-006-0584-8
Fernández-Jiménez, A., Palomo, A. (2005). *Composition and microstructure of alkali activated fly ash binder: Effect of the activator.* Cement and Concrete Research, 35(10), 1984–1992. https://doi.org/https://doi.org/10.1016/j.cemconres.2005.03.003
Hardjito, D., Wallah, S. E., Hardjito, D., Wallah, S. E., Sumajouw, D. M. J., Rangan, B. V. (2005). *Introducing Fly Ash-based Geopolymer Concrete: Manufacture and Engineering Properties.* 30 th Conference on OUR WORLD IN CONCRETE & STRUCTURES, January 2005, 23–24.
Heshmat, M., Amer, I., Elgabbas, F., Khalaf, M. A. (2024). *Effect of binder and activator composition on the characteristics of alkali-activated slag-based concrete*. Scientific Reports, 14(1), 13502. https://doi.org/10.1038/s41598-024-63214-5
Hwang, C. L., Yoon, K. (1981). *Multiple Attribute Decision Making: Methods and Applications. Springer.*
ASTM International. (2018). *Standard Specification for Concrete Aggregates.* In ASTM C33/C33M-18. ASTM International.
ASTM International. (2020). *ASTM C1437-20: Standard Test Method for Flow of Hydraulic Cement Mortar*. ASTM International.
ASTM International. (2022). *Standard Specification for Slag Cement for Use in Concrete and Mortars. In ASTM C989/C989M-22.* ASTM International.
ASTM International. (2023). *ASTM C109/C109M: Standard Test Method for Compressive Strength of Hydraulic Cement Mortars*. ASTM International.
Jolliffe, I. T. (2002). *Principal Component Analysis (2nd ed.).* Springer. https://doi.org/10.1007/b98835
Kaliyavaradhan, S. K., Unnikrishnan, A., Ambily, P. (2024). *CO 2 sequestration through alkali-activated steel slag: a review.* Journal of Sustainable Cement-Based Materials, 14, 1–17. https://doi.org/10.1080/21650373.2024.2434721
Law, D. W., Adam, A. A., Molyneaux, T. K., Patnaikuni, I. (2012). *Durability assessment of alkali activated slag (AAS) concrete.* Materials and Structures/Materiaux et Constructions, 45(9), 1425–1437. https://doi.org/10.1617/s11527-012-9842-1
Liu, M., Dai, W., Jin, W. (2024). *Mix proportion design and carbon emission assessment of high strength geopolymer concrete based on ternary solid waste.* Scientific Reports, 14, 24989. https://doi.org/10.1038/s41598-024-76774-3
Luukkonen, T., Abdollahnejad, Z., Yliniemi, J., Kinnunen, P., Illikainen, M. (2017*). One-part alkali-activated materials: A review.* Cement and Concrete Research, 103. https://doi.org/10.1016/j.cemconres.2017.10.001
Madanchian, M., Taherdoost, H. (2023). *A comprehensive guide to the TOPSIS method for multi-criteria decision making.* Sustainable Social Development, 1(1), 1–6. https://doi.org/10.54517/ssd.v1i1.2220
Marathe, S., Sheshadri, A., Nikolaiev, V. (2025). *Life cycle assessment of sustainable air-cured alkali-activated concrete for permeable pavements using agro-industrial wastes.* Scientific Reports, 15. https://doi.org/10.1038/s41598-025-04783-x
Marvila, M. T., de Azevedo, A. R. G., de Oliveira, L. B., de Castro Xavier, G., Vieira, C. M. F. (2021). *Mechanical, physical and durability properties of activated alkali cement based on blast furnace slag as a function of %Na2O*. Case Studies in Construction Materials, 15(August), e00723. https://doi.org/10.1016/j.cscm.2021.e00723
Mohebi, R., Behfarnia, K., Shojaei, M. (2015). *Abrasion resistance of alkali-activated slag*

concrete designed by Taguchi method. Construction and Building Materials, 98, 792–798. https://doi.org/10.1016/J.CONBUILDMAT.2015.08.128
Nath, P., Sarker, P. K. (2014). *Effect of GGBFS on setting, workability and early strength properties of fly ash geopolymer concrete cured in ambient condition.* Construction and Building Materials, 66, 163–171. https://doi.org/https://doi.org/10.1016/j.conbuildmat.2014.05.080
Provis, J., Deventer, J. (2014). *Alkali Activated Materials: State-of-the-Art Report*, RILEM TC 224-AAM. https://doi.org/10.1007/978-94-007-7672-2
Provis, J. L. (2018). *Alkali-activated materials.* Cement and Concrete Research, 114, 110–120.
Qaidi, S., Najm, H. M., Abed, S. M., Ahmed, H. U., Al Dughaishi, H., Al Lawati, J., Sabri, M. M., Alkhatib, F., Milad, A. (2022). *Fly Ash-Based Geopolymer Composites: A Review of the Compressive Strength and Microstructure Analysis*. Materials, 15(20). https://doi.org/10.3390/ma15207098
Schiefer, C., Plank, J. (2023). *On the CO2 footprint of polycarboxylate superplasticizers (PCEs) and its impact on the eco balance of concrete.* Construction and Building Materials, 409, 133944. https://doi.org/10.1016/j.conbuildmat.2023.133944
Sri Sunarsih, E., As'ad, S., Mohd.Sam, A. R., Kristiawan, S. (2024). *The Effect of Alkali Activator to Binder Ratio on Workability, Density, and Compressive Strength of Fly Ash-Slag Based Geopolymer Mortar.* Nano Hybrids and Composites, 45, 121–127. https://doi.org/10.4028/p-MfE2js
Taguchi, G. (1990). *Introduction to Quality Engineering: Designing Quality into Products and Processes.* Asian Productivity Organization.
Turner, L. K., Collins, F. G. (2013). *Carbon dioxide equivalent (CO2-e) emissions: A comparison between geopolymer and OPC cement concrete.* Construction and Building Materials, 43, 125–130. https://doi.org/10.1016/j.conbuildmat.2013.01.023
Zhang, X. Y., Yu, R., Zhang, J. J., Shui, Z. H. (2022). *A low-carbon alkali activated slag based ultra-high performance concrete (UHPC): Reaction kinetics and microstructure development.* Journal of Cleaner Production, 363, 132416. https://doi.org/https://doi.org/10.1016/j.jclepro.2022.132416
Zheng, Y., Zhong, H., Sun, K., Shen, B., Cui, K., Zhao, Y., Xiong, G., Qin, Q. (2025). *Effect of composite activator on hydration kinetics and micromechanical properties of alkali-activated slag.* Cement and Concrete Composites, 160, 106047. https://doi.org/https://doi.org/10.1016/j.cemconcomp.2025.106047